Novel selenoesters fluorescent liquid crystalline exhibiting a rich phase polymorphism

ARTICLE *in* JOURNAL OF MATERIALS CHEMISTRY · JANUARY 2010

Impact Factor: 7.44 · DOI: 10.1039/B917366H

Novel selenoesters fluorescent liquid crystalline exhibiting a rich phase polymorphism†

Daniel S. Rampon,[a] Fabiano S. Rodembusch,[a] Juliana M. F. M. Schneider,[a] Ivan H. Bechtold,[b] Paulo F. B. Gonçalves,[c] Aloir A. Merlo*[a] and Paulo H. Schneider*[a]

Received 22nd August 2009, Accepted 28th October 2009
First published as an Advance Article on the web 4th December 2009
DOI: 10.1039/b917366h

A simple and efficient procedure for the synthesis of a new class of selenoesters **4a** and **4b** was developed. Polarized-light optical microscopy (POM), differential scanning calorimetry (DSC), and X-ray diffraction showed that the selenoester **4a** with a shorter alkyl chain displayed a wide nematic range ($\Delta T = 110.7$ °C), while **4b** with a longer alkyl chain possesses a rich phase polymorphism: Cr → SmI → SmC → N → I mesophase sequence during heating cycle and I → N → SmC → SmI → SmX → Cr transition on cooling. For **4b**, a large temperature range (135.7 °C) from crystal to isotropic phase can be observed. In addition, UV-Vis, steady-state fluorescence emission and excitation spectra in solution were also applied in order to characterize their photophysical behaviour. Compounds **4a** and **4b** are fluorescent in the blue region and present a Stokes shift at around 80 nm and 39 nm in dichloromethane and dioxane, respectively.

Introduction

Organoselenium chemistry has made great advances during the last decades. Selenium compounds have found wide uses due to their unique properties in a number of different reactions.[1] In addition, they have become attractive synthetic targets because of their chemo- and regioselective reactions,[2] tolerating a large variety of functional groups, thus avoiding protection group chemistry. More recently, selenium containing compounds have been used as chiral catalysts or as chiral ligands in various stereoselective reactions.[3] The biological and medicinal properties of selenium and organoselenium compounds are increasingly appreciated, mainly due to their antioxidant, antitumor, antimicrobial and antiviral properties.[4] Besides, the synthesis of peptides containing selenocysteine is rapidly gaining interest with the discovery of an increasing number of proteins containing this amino acid.[5]

Chalcogen derivatives have also been intensively studied because of their excellent electrical properties. For instance, chalcogenophene oligomers are compounds of current interest since many of them show photo enhanced biological activities[6] and the alpha-types, such as 5,2′:5′,2″-terthiophene, produce crystalline electroconductive polythiophenes in electrochemical polymerizations.[7] Thus, a wide variety of oligomers and related chalcogen compounds including mixed thiophene–pyrrole have been synthesized mainly with the expectation of obtaining excellent precursor compounds for molecular devices and electrocondutive polymers. In the area of semiconductors, liquid crystals containing chalcogen atoms such as hexaalkylthiotriphenylenes and dithienyl acene derivatives, show fast mobilities of charge carriers in the mesophases of 10^{-1}–10^{-2} cm^2 V^{-1} s^{-1}.[8] Moreover, earlier studies, have shown that different chalcogen atoms in a series of compounds can also induce changes in their photophysical properties.[8] Among chalcogenides, the selenoesters play an important role in organic synthesis, having been used as key intermediates in several organic transformations.[2,9]

However, the examples where selenium compounds, especially selenoesters, are reported as liquid crystalline materials are rare,[10] despite their promising photophysical properties for optical device applications such as emissive LC displays, polarized organic lasers and anisotropic OLEDs.

In this paper we wish to report the design and synthesis of a new class of selenoesters in a straightforward manner which allows us to explore the effects of the selenium atom on the stability and packing order in the mesophases as well as on their photophysical behavior. To the best of our knowledge this is the first time that these types of selenoesters have been investigated concerning their liquid crystalline and fluorescent properties. These compounds are fluorescent in the blue region and exhibit their stability and liquid crystalline properties over a large range of temperatures.

Results and discussion

Scheme 1 outlines the synthesis of the key intermediate **3** starting with the preparation of the acetylene **1**, the synthesis of which has been described previously.[11] Thus the alkylation of *p*-bromophenol with 1-bromooctane gave the corresponding alkylaryl ether in 81% yield. A Sonogashira reaction[12] of the alkylaryl ether with 2-methyl-3-butyn-2-ol (mebynol), followed by deprotection using KOH and isopropanol furnished the acetylene **1**.[13] Finally, through a second Sonogashira reaction of the

[a]*Instituto de Química, Universidade Federal do Rio Grande do Sul, UFRGS, C.P. 15003, 9150-970 Porto Alegre-RS, Brazil. E-mail: paulos@iq.ufrgs.br; Fax: +55 51 3308 7304; Tel: +55 51 3308 6286*
[b]*Departamento de Física, Universidade Federal de Santa Catarina –UFSC, 88040-900 Florianópolis-SC, Brazil*
[c]*Instituto de Química, Centro Universitário La Salle, Av. Victor Barreto, 2288. Centro, 92010-000 Canoas, RS, Brasil*

† Electronic Supplementary Information (ESI) available: Details ^{1}H and ^{13}C NMR spectra, DSC, POM microscopy. See DOI: 10.1039/b917366h/

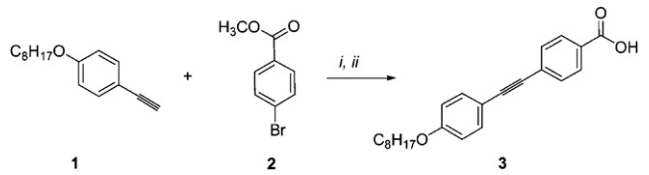

Scheme 1 Synthesis of the key intermediate **3**. Reaction conditions: *i*. $PdCl_2(PPh_3)_2$, Et_3N, CuI, PPh_3 (48%); *ii*. KOH 1M, THF, reflux, then HCl conc. (68%)

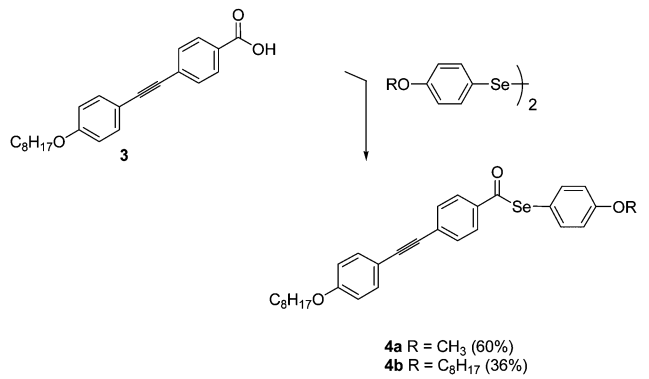

Scheme 2 Synthesis of selenoesters LC **4a** and **4b**. Reaction conditions: PBu_3, DCM, r.t.

acetylene derivative **1** and methyl 4-bromobenzoate **2**, compound **3** was obtained after hydrolysis in satisfactory yields.

Having obtained the acid **3**, we concentrated our efforts on the synthesis of the target molecules. The selenium group can be introduced in an organic substrate *via* both nucleophile and electrophile reagents. There are some established methods to obtain selenoesters by treating acylhalides with indium salts and diselenides,[14] or by reacting carboxylic acids with tributylphosphine and a dichalcogenide.[15] In this way, the resulting acid **3** was converted into selenoesters **4a,b** by arylselenation as reported by Batty and Crich[15b] (Scheme 2). Both final products were characterized by spectroscopic means and their structures are consistent with the spectral data and elemental analysis.

Phase transition behavior

The thermal behavior of the selenoesters-LC was investigated by means of polarizing optical microscopy (POM), differential scanning calorimetry (DSC), and X-ray diffractometry. The transition temperatures and enthalpy values (kcal mol^{-1}) of the selenoesters-LC **4a** and **4b** are presented in Table 1. The relevant pictures of the mesophase investigated in this work as well as the DSC thermograms are collected in Fig. 1–3. The DSC thermograms clearly indicate the presence of two endothermic peaks for LC **4a** and four endothermic peaks for LC **4b** during heating cycles. On cooling, the DSC trace of **4a** displays the same behavior as seen in its heating cycle. However, **4b** displays a fifth peak during the cooling cycle. In both selenoesters-LC there is a hysteresis during the cooling cycle at approximately 11.0 °C. The temperature hysteresis of recrystalization of **4b** allows the appearance of an additional monotropic smectic phase observed

Table 1 Phase transition temperatures (°C) for selenoesters-LC **4a,b** and enthalpy values (ΔH, kcal mol^{-1})

LC	Cycle	Phase sequence	ΔT^a
4a	Heating	Cr 108.1 N 218.8 I	110.7
	Cooling	I 216.1 N 97.0 Cr	
	Enthalpies[b]	Cr 5.00 N 0.11 I	
4b	Heating	Cr 66.8 SmI 121.7 SmC 163.3 N 202.5 I	135.7
	Cooling	I 199.7 N 159.7 SmC 118.7 SmI 62.3 SmX 53.2 Cr	
	Enthalpies[b]	Cr 7.52 SmX 0.31[c] SmI 0.63 SmC 0.08 N 0.29 I	

[a] Total value. [b] On heating. [c] Enthalpy values obtained from cooling cycle.

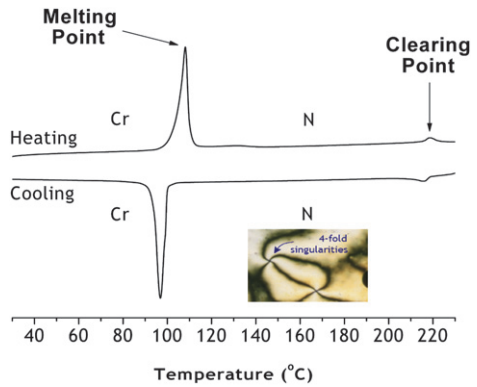

Fig. 1 DSC traces of selenoester-LC **4a** for rates of 10 °C min^{-1}; 2nd heating and cooling runs are shown; Cr – crystal phase; N – nematic phase; I – isotropic phase.

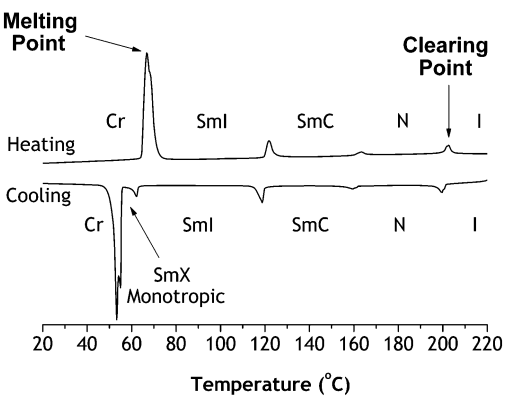

Fig. 2 DSC curves of selenoester-LC **4b** for rates of 10 °C min^{-1}; 2nd heating and cooling runs are shown. Cr – crystal phase; N – nematic phase; SmC – smectic C phase; SmI – smectic I phase; SmX – smectic X phase; I – isotropic phase.

in the DSC trace at 62.3 °C. The mesophase textures were assigned in the cooling mode.

Selenoester **4a** only displays the nematic phase which is expected for derivatives with short alkyl chains. The DSC trace of **4a** showed two reversible peaks (Fig. 1) which is in accordance with the analysis of the texture and the transition temperature observed by polarized optical microscopy. On cooling, the

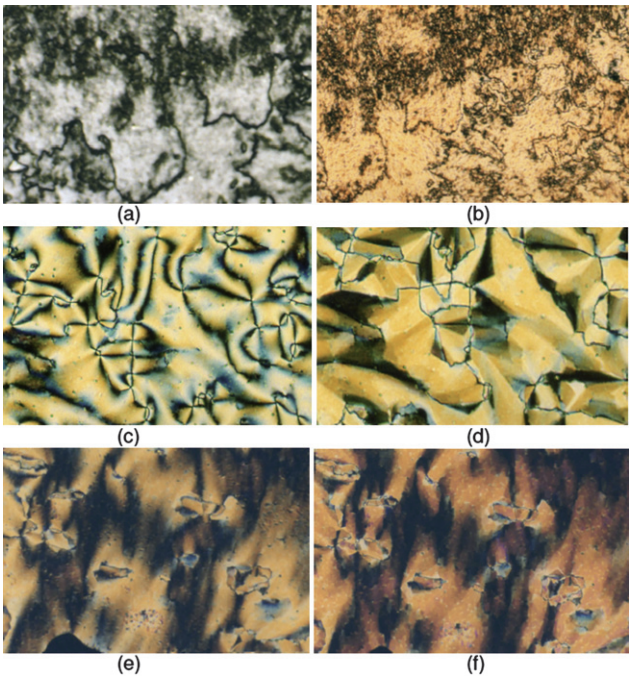

Fig. 3 Optical micrographs between crossed polarizers of selenoester-LC **4b**: (a) planar thread-like nematic texture occurring at 164 °C; (b) schlieren texture grainy at 144 °C of the smectic C phase; (c) schlieren type texture of smectic I phase with loops of disclination lines at 105 °C; (d) paramorphotic mosaic texture of the smectic I at 82 °C; (e) mosaic texture of the smectic I at 100 °C; (f) mosaic texture of the smectic X at 58 °C.

isotropic liquid enters into a nematic phase for a large temperature range (ΔT = 110.7 °C). The wide temperature range (>100 °C) over which the nematic phase is stable for **4a** is striking (Table 1). The enthalpy value of 0.11 kcal mol^{-1} for the N phase to isotropic phase is consistent with a less ordered nematic mesophase. An illustration of nematic phase texture found in **4a** is inserted at the right corner of Fig. 1, in which a schlieren texture was clearly observed as indicated by the point where the four dark brushes meet.

The superior homologous **4b** exhibited very rich smectic polymorphism, as shown in Table 1 and in Fig. 2 and 3. The POM and DSC data revealed that **4b** is a liquid crystal exhibiting four peaks and three mesophases during the heating cycle and, five peaks with four mesophases on cooling. These peaks are associated with the transitions I → N at 199.7 °C; N → SmC at 159.7 °C; SmC → SmI at 118.8 °C; SmI → SmX at 62.3 °C; SmX → Cr at 53.2 °C. Selenoester **4b** surprisingly displays three tilted smectic phases. The appearance of a tilted smectic, *e.g.*, smectic C, smectic I and smectic X phases in this compound is a consequence of the longer alkyl chains effect on the terminal position at the phenyl group.[16]

On cooling, the isotropic melts and **4b** undergoes a transition with a small enthalpy change (Table 1). The sample below this transition temperature is very fluid and birefringent exhibiting a planar thread-like nematic texture as we can see in Fig. 3a. X-Ray diffraction scans recorded in this phase showed only broad and diffuse peaks confirming that **4b** self-organizes into the nematic phase. On cooling further, **4b** undergoes a three phase transition consecutively. Below the nematic transition temperature, this compound displays a typical schlieren texture of smectic C phase (Fig. 3b). Enthalpy value of 0.08 kcal mol^{-1} associated with this phase transition suggests a first-order transition going from nematic to smectic C phase. When the sample passes by the SmC–SmI phase transition, a sudden change of schlieren texture is observed (Fig. 3b→c). The defect points and the disclination lines become clear and with better resolution. In Fig. 3d, we can see a large mosaic formed of smectic I phase at 82.0 °C. The enthalpy value for this transition of 0.63 kcal mol^{-1} is high and represents an increase in the local order of this phase. A further decrease of temperature induced the fourth mesophase, as shown in the DSC traces (Fig. 2) with enthalpy values of 0.31 kcal mol^{-1}. At crossed polarizers, a small change in mosaic texture can be visualized inside the domains through this transition. However, on cooling, the sample is more birefringent as noted by the continuous change of colors inside the domain (Fig. 3e → 3f). This behavior suggests a smectic liquid crystalline nature that was confirmed by powder X-ray diffraction measurements of **4b**, where the inter-layer distance remains constant at 32.8 ± 1 Å. This mesophase was assigned as smectic X

The X-ray diffraction experiment was carried out on compound **4b**to investigate its smectic phases. All the patterns recorded contain a sharp peak in the low-angle region, arising from the reflection of the X-ray beam on the smectic layers, and their corresponding higher order peaks. The inter-layer spacing was obtained by applying Bragg's law to the first maximum.

Fig. 4 shows the pattern of compound **4b** in the SmC phase at 150 °C and a smectic phase at 80 °C, where in both cases the

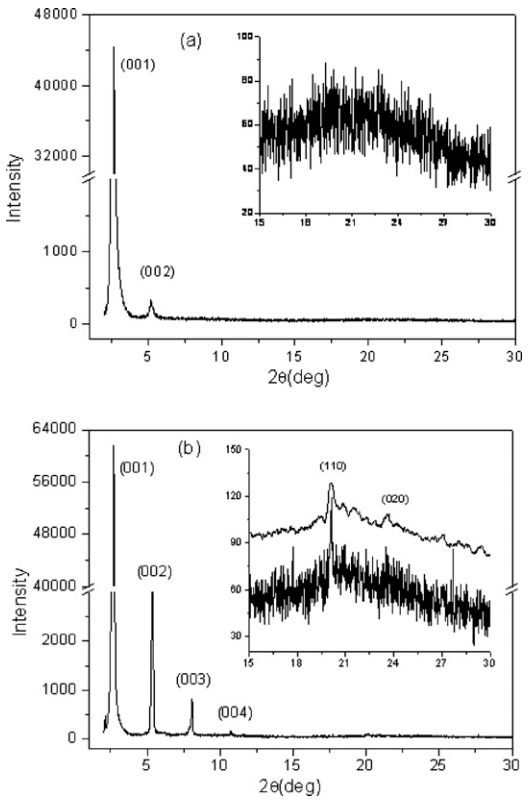

Fig. 4 X-Ray diffraction patterns of compound **4b**, with indication of the Miller indices. (a) SmC phase at 150 °C and (b) smectic phase at 80 °C. Inset we emphasize the wide-angle region.

smectic order was confirmed by the ratio of the value obtained for the inter-layer spacing related to (001) with respect to the higher order peaks. It is well known that this ratio must obey the relation 1 : 2 : 3 : 4… in smectic phases.

The higher diffracted intensity of the peaks and the appearance of more secondary peaks indicate that the smectic phase at 80 °C is more organized and propagates to longer distances in the medium. The X-ray results show that the organization of the smectic phases increases with the reduction of the temperature, and that the smectic order is preserved even after the solidification takes place (see the spectrum collected at 30 °C after solidification in the ESI†).

The inset of Fig. 4(a) and 4(b) show in detail the broad diffuse band centered around 4.1 Å, which is related to the liquid-like order between the aliphatic chains. In Fig. 4(b) it is possible to observe the appearance of two additional peaks in this region, which could be interpreted in the sense of a SmI phase as the (110) and (020) reflections of a monoclinic unit cell within one layer[17] (the upper line was smoothed to reduce the noise). From Bragg's law, $d_{110} = 4.4$ Å and $d_{020} = 3.8$ Å, where these distances correspond to the intraplanar hexatic order exhibited by this phase.

It is important to discuss the interpretation of a SmI phase instead of a SmF phase, due to the fact that the last one is also characterized by two peaks (110) and (020) in the same region. The inter-layer spacing was calculated for several diffractograms collected at specific temperatures during the cooling process, where Fig. 5 shows the obtained values as a function of the temperature.

As SmI represents a hexatic phase tilted towards the apex of the hexagon, at the SmC–SmI transition the molecules preserve the same inter-planar distance, and this distance decreases a little across the SmI phase until the transition to the SmX takes place. According to the literature, a SmC to SmF transition is usually accompanied by a discontinuous jump in the layer spacing,[18] which is not observed here. At the SmI–SmX transition a discontinuous increase of the inter-layer spacing occurs. The smectic layers of the SmX phase exhibit approximately the same distance of the SmC, which is constant during the SmX range. A significant inter-layer distance increase is observed at the SmX–Cr phase transition, after that it remains constant at 35.5 ± 1 Å. Therefore, our data strongly suggest the existence of a SmI phase when cooling down from the SmC.

The molecular length was obtained by quantum mechanical calculations carried out for systems using the Gaussian 03 program.[19] The molecular geometry was obtained from DFT calculations using 6-31G(d,p) basis functions and B3LYP hybrid functional. The molecule length was calculated considering the distances between the far atoms with the addition of the van der Waals radii from hydrogen atoms bonded to the first and last carbon atoms in the chain (Fig. 6). The value for the fully extended all *trans*-conformation is $l = 42.9$ Å. By considering l as the length adopted by the molecules in the smectic layers it is possible to calculate the tilt angle (θ) with the equation: $\theta = \cos^{-1}[d_m/l]$, where d_m is the inter-layer spacing measured with the X-ray experiments. In the SmC phase $\theta_{SmC} = 40.5°$, in the SmI phase θ_{SmI} varies from 40.5° (at 110 °C) to 41.6° (at 60 °C) and in the SmX phase $\theta_{SmX} = 40.1°$. In practice, the molecules do not adopt the most extended configuration in the smectic layers due to conformational disorder of the aliphatic chains, and l can be reduced from 2.4 Å to 5.6 Å.[20] With this consideration, θ_{SmC} may have its value reduced to 30°. Thus, the tilted smectic layers of this compound can present tilt angles between 30° and 42°.

Photophysical characterization

Fig. 7 shows the normalized UV-Vis absorption spectra of these selenoesters **4a** and **4b** in dichloromethane and dioxane. The relevant UV-Vis data are summarized in Table 2.

An absorption band maxima (λ_{max}^{abs}) located around 340 nm, with molar extinction coefficient values (ε_{max}) in agreement with π–π* transitions, could be observed to the dyes in dichloromethane and dioxane. The different alkyl groups in the selenoester moieties do not play a fundamental role in the absorption process, since any significant solvatochromic effect (<3 nm)

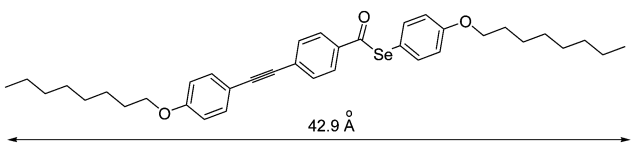

Fig. 6 Dimensions of molecular structure of selenoester LC **4b** estimated from simulation.

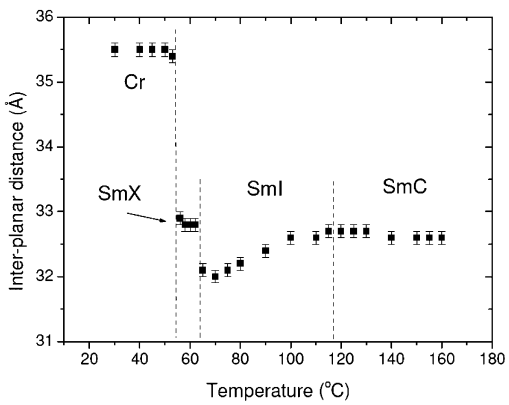

Fig. 5 Inter-layer spacing as a function of the temperature across the smectic phases until the solidification for selenoester **4b**.

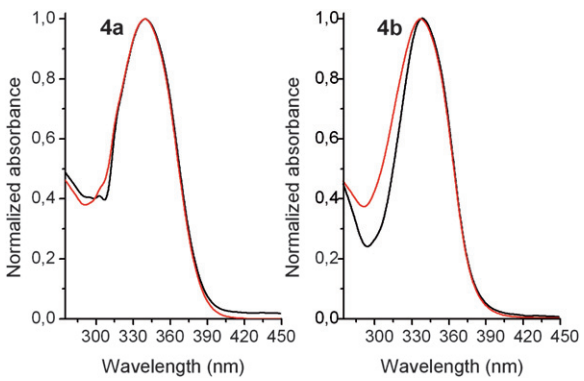

Fig. 7 Normalized absorption spectra of selenoesters LC **4a** and **4b** in dichloromethane (red line) and dioxane (black line).

Table 2 UV-Vis absorbance and fluorescence emission data of the selenoesters-LC **4a** and **4b**

LC	Solvent	(λ_{max}^{abs})/ nm	$\varepsilon_{max} \times 10^{-4}$/l mol^{-1} cm^{-1}	(λ_{max}^{em})/ nm	(λ_{max}^{exc})/ nm	$(\Delta\lambda_{ST})$/ nm	ϕ_{fl}
4a	DCM	340	4.6	413	320	73	0.1
	Dioxane	339	1.8	364	307	25	0.05
4b	DCM	339	4.8	428	333	89	0.1
	Dioxane	337	4.3	392	325	55	0.05

could be observed in the absorption curves between **4a** and **4b**. The higher ε_{max} values indicate very planar structures which are related to the tolane portion.

Fig. 8 and 9 show the normalized fluorescence emission and excitation spectra in dichloromethane and dioxane, respectively. The curves were obtained using the absorption maxima as the excitation wavelengths. The relevant data are summarized in Table 2.

The selenoesters-LC **4a** and **4b** in dichloromethane present a main emission band located between 410 and 428 nm. A Stokes shift higher than 73 nm was observed for these molecules. Comparing the obtained UV-Vis curves (Fig. 7) with the presented fluorescence spectra in Fig. 8, a mirror image of the absorption can be observed, indicating that the fluorescence is emitted from the excited state which gives the maximum absorption wavelength.[21]

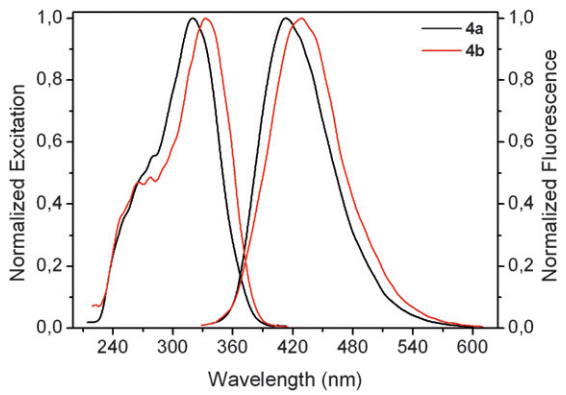

Fig. 8 Normalized excitation and emission spectra of the selenoesters-LC **4a** and **4b** in dichloromethane.

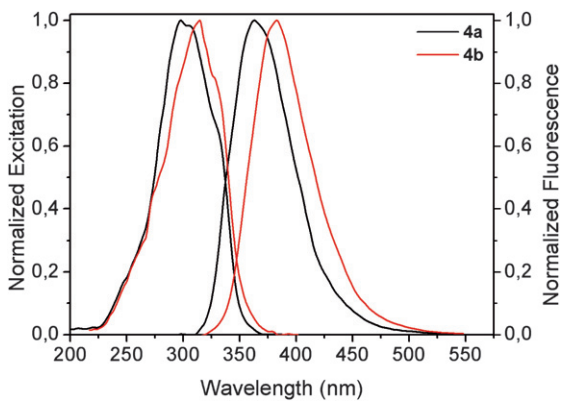

Fig. 9 Normalized excitation and emission spectra of the selenoester-LC **4a** and **4b** in dioxane.

The fluorescence excitation spectra also present a main emission band located between 320 and 333 nm. With few exceptions, the fluorescence excitation spectrum of a single fluorescent dye in dilute solution is identical to its absorption spectrum. Note that the excitation spectra (Fig. 8) are quite similar to the UV-Vis absorption curves (Fig. 7). However, the excitation maxima are blue shifted by 6–20 nm to the respective absorption. Since the excitation signal, although proportional to the molecule absorbance, is not the absorption of the whole molecule as observed in the UV-Vis spectra. The observed blue shift can be probably related to the absorption of such part of the molecule which is responsible for the emission.[22]

It can also be observed that **4b** presents red shifted excitation and emission bands in comparison to **4a**, indicating loss of energy by non radiactive paths in the excited state, which is probably due to the length differences of the alkyl groups. A higher chain length ($-OC_8H_{17}$) can present more deactivation states without quenching the fluorescence emission despite the methoxy group ($-OCH_3$) in the selenoester LC **4a**.

Fig. 9 depicts the photophysical behavior of the dyes in dioxane, where one main fluorescence emission band located at 364 and 392 nm can be observed to the selenoesters-LC **4a** and **4b**, respectively. A lower Stokes shift (~40 nm) in relation to those in dichloromethane was observed for these molecules. This result indicates that the dipole moment of the dyes are higher in the excited state than in the ground state, since the Stokes shift increases with the solvent polarity.[22] Higher values of the quantum yields were obtained in dichloromethane, which indicates a stronger interaction between the dyes and the dioxane, resulting in non radiation processes. In both solvents, the methoxy group attached to aromatic ring does not play a fundamental role on the quantum yield values.

Conclusions

In summary, we have shown a practical and concise synthesis of a new class of selenoester fluorescent liquid-crystals by an easy, straightforward and flexible synthetic route. The thermotropic liquid crystalline properties were investigated by DSC, POM and XRD analysis. The final selenoester-LC **4a** exhibited a stable and large nematic mesophase range. To the selenoester-LC **4b**, a rich and stable polymorphism N–SmC–SmI–SmX was found. In addition, selenoester LC **4a** and **4b** are fluorescent in the blue region and present a Stokes shift higher than 39 nm.

Experimental

General

4-Bromophenol, 1-bromoalkanes, 2-methyl-3-butyn-2-ol (mebynol), KOH, triphenylphosphine (PPh_3), tributylphosphine (PBu_3), CuI, dimethylformamide (DMF), benzene, ethanol and 4-bromobenzoic acid were used without further purification from Aldrich. Triethylamine was distilled over KOH and isopropanol and dichloromethane distilled over CaH_2 under argon immediately prior to use. All other commercial solvents and reagents were used without further purification. The reactions

were accompanied by analytical thin-layer chromatography (TLC), conducted on Merck aluminium plates with 0.2 mm of silica gel 60 F_{254}. The melting points and mesophase transition temperatures and textures of the samples were measured on a Mettler Toledo FP82HT Hot Stage FP90 Central Processor and DSC Q2000 Series TA Instruments. Nuclear magnetic resonance spectra were obtained on a Varian 300 MHz instrument. Chemical shift are given in parts per million (δ) and are referenced from tetramethylsilane (TMS). CHN analyses were performed on a Perkin-Elmer 2400 CHN Elemental Analyzer.

X-Ray experiments

The X-Ray diffraction experiments were realized with an X'Pert-PRO (PANalytical) diffractometer system using the linear monochromatic Cu $K\alpha_1$ beam ($\lambda = 1.5405$ Å), with an applied power of 1.2 kV A. The scans were performed in continuous mode from 2° to 30° (2θ angle) and the diffracted radiation collected with an X'Celerator detector. The sample of selenoester LC **4b** was prepared by a previous heating (with a hot stage) of an amount of powder on a glass plate until the isotropic phase at 205 °C, followed by a cooling process until the solidification takes place. As a result we obtained a film about 1 mm thick. The film was then placed in the diffractometer chamber on the TCU2000 - Temperature Control Unit (Anton Paar), which allows a precise control of the sample temperature during the measurement. The film was first heated until the nematic phase (at 190 °C) and the diffraction patterns collected during the cooling for different temperatures across the smectic phases until the solidification. We used a rate of 5 °C min^{-1} and waited 2 min after each cooling step.

Photophysical experiments

Spectroscopic grade solvents (Merck) were used for fluorescence and excitation spectra and UV-Vis absorption spectroscopy measurements. UV-Vis absorption spectra were recorded on a Shimadzu UV-1601PC spectrometer. Fluorescence emission and excitation spectra were measured on a Hitachi spectrofluorometer model F-4500. Spectrum correction was performed to enable measurement of a true spectrum by eliminating instrumental response such as wavelength characteristics of the monochromator or detector using rhodamine B as an internal standard (quantum counter). All the experiments were performed at room temperature in a concentration range 10^{-5}–10^{-6} M. The quantum yield of fluorescence (ϕ_{fl}) was made at 25 °C in spectroscopic grade solvents in a solution with an absorbance intensity lower than 0.05. Quinine sulfate (Riedel) in H_2SO_4 1 M ($\phi_{fl} = 0.55$) was used as the quantum yield standard.[23,24]

Synthesis

1-Ethynyl-4-(octyloxy)benzene (1)

Alkylation Reaction.[11c]. 4-Bromophenol (26 g, 150 mmol) and potassium hydroxide (10 g, 178 mmol) were added to benzene and DMF (1 : 1, 200 mL) and heated at 50 °C for 15 min. Then, *n*-octylbromide (31 mL, 178 mmol) was added dropwise and the mixture heated under reflux for 6 h. The solid formed was filtered off and the filtrate concentrated. The residue was dissolved in diethyl ether (200 mL), washed with 10% sodium bicarbonate solution (2 × 100 mL), and water (100 mL), then dried over anhydrous sodium sulfate. The solvent was removed by evaporation and the product purified by distillation under reduced pressure. The compound was obtained as pale yellow viscous liquid.

Yield: 34.6 g, 81%; bp 117 °C (1 mmHg). ^{1}H NMR ($CDCl_3$): $\delta = 0.88$ (t, 3H, CH_3), 1.28 (m, 10H, $(CH_2)_5$), 1.72 (m, 2H, CH_2CH_2O), 3.83 (t, $J = 6.5$ Hz, 2H, CH_2O), 6.71 (d, $J = 8.9$ Hz, 2H, Ar), 7.3 (d, $J = 8.9$ Hz, 2H, Ar); ^{13}C NMR ($CDCl_3$): $\delta =$ 14.03, 22.6, 25.9, 29.1, 29.2, 29.3, 31.7, 68.1, 112.4, 116.1, 117.2, 132, 132.2, 158.1.

Sonogashira Coupling Reaction.[11c]. A test tube was charged with Et_3N (100 mL), 2-methyl-3-butyn-2-ol (7 mL, 70 mmol), and 1-bromo-4-(octyloxy)benzene (9 g, 32 mmol) under argon. To the solution were added CuI (216 mg), PPh_3 (123 mg), and $PdCl_2(PPh_3)_2$ (69 mg). The mixture was heated for 24 h at 90 °C. After cooling, the solid was filtered and washed with CH_2Cl_2 (100 mL). The filtered mixture was evaporated, and the resulting dark yellow oil was dissolved in CH_2Cl_2 (200 mL) and washed with water (3 × 80 mL), cold 5 N hydrochloric acid (80 mL), and water (80 mL). The organic layer was dried over anhydrous sodium sulfate. The solvent was evaporated and the remaining solid was purified by chromatography. A yellow solid was obtained in 42% yield.

Yield: 3.8 g, 42%; mp 60.2 °C. ^{1}H NMR ($CDCl_3$): $\delta = 0.89$ (t, 3H, CH_3), 1.3 (m, 10H, $(CH_2)_5$), 1.6 (s, 6H, CH_3), 1.8 (m, 2H, CH_2CH_2O), 2.2 (s, 1H, OH), 3.9 (t, $J = 6.6$ Hz, 2H, CH_2O), 6.8 (d, $J = 8.8$ Hz, 2H, Ar), 7.3 (d, $J = 8.8$ Hz, 2H, Ar). ^{13}C NMR ($CDCl_3$): $\delta = 14.0$, 22.6, 25.9, 29.1, 29.2, 29.3, 31.5, 31.8, 65.7, 68.0, 76.6, 77.0, 77.4, 82.1, 92.2, 114.4, 114.5, 133.0, 159.1.

4-[4-(Octyloxyphenylethynyl)]benzoic acid (3)

Deprotection and Coupling Reaction.[11c]. Potassium hydroxide (0.5 g, 9 mmol) and isopropanol (40 mL) were added to a round bottomed flask and heated at 50 °C for 15 min. Then, a solution of 4-(4-octyloxyphenyl)-2-methylbut-3-yn-2-ol (0.9 g, 3 mmol) in isopropanol (10 mL) was added. The mixture was heated under reflux for 2 h. The solvent was evaporated, the residue dissolved in CH_2Cl_2 (50 mL), and washed with water (3 × 30 mL). The organic layer was dried over anhydrous sodium sulfate. The solvent was evaporated and a yellow oil was obtained in 99% yield. This oil was used for another Sonogashira coupling with methyl 4-bromobenzoate. After cooling of the reaction test tube, the solid was filtered and washed with CH_2Cl_2 (100 mL). The filtered mixture was evaporated, and the resulting dark yellow oil was dissolved in CH_2Cl_2 (200 mL) and washed with water (3 × 80 mL), cold 5 N hydrochloric acid (80 mL), and water (80 mL). The organic layer was dried over anhydrous sodium sulfate. The solvent was evaporated and the remaining solid was purified by chromatography and recrystallization from hexane.

Yield: 1.79 g, 48%; mp 112.6 °C. ^{1}H NMR ($CDCl_3$): $\delta = 0.89$ (t, 3H, CH_3), 1.3 (m, 10H, $(CH_2)_5$), 1.8 (m, 2H, CH_2CH_2O), 3.92 (s, 3H, CH_3O), 3.97 (t, $J = 6.6$ Hz, 2H, CH_2O), 6.9 (d, $J = 8.8$ Hz, 2H, Ar), 7.4 (d, $J = 8.8$ Hz d, 2H, Ar), 7.6 (d, $J = 8.1$ Hz, 2H, Ar), 8.0 (d, $J = 8.1$ Hz, 2H, Ar). ^{13}C NMR ($CDCl_3$): $\delta = 14.1$, 22.7, 26.0, 29.1, 29.2, 29.3, 31.8, 52.2, 68.1, 77.2, 87.4, 92.7, 114.4, 114.6, 128.5, 129.0, 129.5, 131.3, 133.2, 159.6, 166.6.

Hydrolysis Reaction[25]. Methyl-4-(4-octyloxyphenylethynyl) benzoate (0.8 g, 2.3 mmol) was dissolved in THF (30 mL) and 1 M aq KOH (12 mL) was added. After heating the reaction mixture at 60 °C for 24 h, the resulting solution was evaporated to dryness. The solid was dissolved in water (60 mL) and then the aqueous solution was acidified by conc HCl (pH = 1). White precipitate was filtered, washed with water, and then dried. The product was obtained by recrystallization from EtOH.

Yield: 0.6 g, 68%; dc > 250 °C. ^{1}H NMR (DMSO-d6): $\delta = 0.89$ (t, 3H, CH_3), 1.3 (m, 10H, $(CH_2)_5$), 1.7 (m, 2H, CH_2CH_2O), 2.5 (s, 1H, OH), 4.0 (t, $J = 6.4$ Hz, 2H, CH_2O), 7.0 (d, $J = 8.6$ Hz, 2H, Ar), 7.5 (d, $J = 8.8$ Hz, 2H, Ar), 7.6 (d, $J = 8.2$ Hz, 2H, Ar), 8.0 (d, $J = 8.2$ Hz, 2H, Ar). ^{13}C NMR (DMSO-d_6): $\delta = 13.6$, 21.7, 25.2, 28.3, 28.3, 28.4, 30.9, 67.5, 87.1, 92.1, 113.4, 114.8, 126.9, 129.2, 130.0, 130.9, 132.9, 159.2, 164.0, 166.4.

4-Methoxyphenyl-4-[(4-octyloxyphenyl)ethynyl]-benzoselenoate (4a). Tributylphosphine (0.15 mL, 0.6 mmol) was slowly added to dichalcogenide (0.3 g, 0.8 mmol) in anhydrous CH_2Cl_2 (30 mL) and the mixture left to stir for 15 min. 4-(4-(octyloxyphenylethynyl)benzoic acid (**3**) (0.14 g, 0.4 mmol) was then added and the reaction stirred for 24 h at room temperature until no precipitate was visible. The reaction mixture was diluted with CH_2Cl_2 and washed with water (50 mL), sat. sodium bicarbonate (2 × 50 mL), and water (50 mL). The organic layer was dried over anhydrous sodium sulfate. The solvent was evaporated and the remaining solid was purified by chromatography and recrystallization from hexane.

Yield: 0.1 g, 50%; Cr 118.1 °C N 218.8 °C I. ^{1}H NMR ($CDCl_3$): $\delta = 0.89$ (t, 3H, CH_3), 1.3 (m, 10H, $(CH_2)_5$), 1.8 (m, 2H, CH_2CH_2O), 3.85 (s, 3H, CH_3O), 3.98 (t, $J = 6.6$ Hz, 2H, CH_2O), 6.9 (d, $J = 8.6$ Hz, 2H, Ar), 7.0 (d, $J = 8.5$ Hz d, 2H, Ar), 7.48 (d, $J = 8.6$ Hz, 2H, Ar), 7.50 (d, $J = 8.4$ Hz, 2H, Ar). 7.6 (d, $J = 8.2$ Hz, 2H, Ar), 7.9 (d, $J = 8.1$ Hz, 2H, Ar). ^{13}C NMR ($CDCl_3$): $\delta =$ 14.8, 23.3, 26.7, 29.8, 29.9, 29.9, 30.0, 32.5, 56.0, 68.8, 88.0, 94.3, 115.0, 115.3, 115.9, 116.7, 127.9, 130.2, 132.4, 134.0, 137.8, 138.5, 160.4, 161.2, 194.2 Anal. calcd. for $C_{30}H_{32}O_3Se$: C, 69.35; H, 6.21, found: C, 68.95; H, 6.65.

4-Octyloxyphenyl-4-[(4-octyloxyphenyl)ethynyl]-benzoselenoate (4b). An experimental procedure identical to that used for the preparation of **4a** was applied.

Yield: 0.17 g, 36%; Cr 66.8 °C SmI 121.7 °C SmC 163.3 °C N 202.5 °C I. ^{1}H NMR ($CDCl_3$): $\delta = 0.81$ (m, 6H, 2 × CH_3), 1.4 (m, 20H, 2 × $(CH_2)_5$), 1.7 (m, 4H, 2 × CH_2CH_2O), 3.9 (m, $J = 6.6$ Hz, 4H, 2 × CH_2O), 6.80 (d, $J = 8.8$ Hz, 2H, Ar), 6.85 (d, $J = 8.8$ Hz d, 2H, Ar), 7.38 (d, $J = 8.8$ Hz, 2H, Ar), 7.39 (d, $J = 8.8$ Hz, 2H, Ar), 7.5 (d, $J = 8.4$ Hz, 2H, Ar), 7.8 (d, $J = 8.4$ Hz, 2H, Ar). ^{13}C NMR ($CDCl_3$): $\delta = 14.8$, 23.4, 26.7, 26.7, 29.8, 29.9, 29.9, 30.0, 32.5, 32.5, 68.7, 68.8, 77.3, 77.7, 78.1, 88.1, 94.3, 115.0, 115.3, 116.3, 116.4, 127.9, 130.1, 132.4, 134.0, 137.8, 138.4, 160.4, 160.8, 194.2. Anal. calcd. for $C_{37}H_{46}O_3Se$: C, 71.94; H, 7.51, found: C, 72.54; H, 7.90.

Acknowledgements

We are grateful to the CAPES, CNPq, INCT-CMN and FAPERGS for financial support. CAPES is also acknowledged for master fellowship for D. S. R. The X-ray diffraction experiments were performed at the Laboratório de Difração de Raios-X (LDRX-DF/UFSC).

References

1 G. Zeni, D. S. Lüdtke, R. B. Panatieri and A. L. Braga, *Chem. Rev.*, 2006, **106**, 1032; G. Zeni, A. L. Braga and H. A. Stefani, *Acc. Chem. Res.*, 2003, **36**, 731.
2 Organoselenium Chemistry. T. Wirth, in *Topics in Current Chemistry 208*, Springer-Verlag, Heidelberg, 2000; A. Krief, in *Comprehensive Organometallic Chemistry II*, ed. E. V. Abel, F. G. A. Stone, G. Wilkinson, Pergamon Press, New York, 1995, vol. 11. (chapter 13); C. Paulmier, Selenium Reagents and Intermediates in Organic Synthesis, in *Organic Chemistry Series 4*, ed. J. E. Baldwin, Pergamon Press, Oxford, 1986.
3 Some examples: T. Wirth, *Tetrahedron Lett.*, 1995, **36**, 7849; C. Santi and T. Wirth, *Tetrahedron: Asymmetry*, 1999, **10**, 1019; A. L. Braga, M. W. Paixão, D. S. Lüdtke, C. C. Silveira and O. E. D. Rodrigues, *Org. Lett.*, 2003, **5**, 2635; A. L. Braga, S. J. N. Silva, D. S. Lüdtke, R. L. Drekener, C. C. Silveira, J. B. T. Rocha and L. A. Wessjohann, *Tetrahedron Lett.*, 2002, **43**, 7329; A. L. Braga, C. C. Silveira, M. W. G. de Bolster, H. S. Schrekker, L. A. Wessjohann and P. H. Schneider, *J. Mol. Catal. A: Chem.*, 2005, **239**, 235; A. L. Braga, M. W. Paixão, B. Westermann, P. H. Schneider and L. A. Wessjohann, *J. Org. Chem.*, 2008, **73**, 2879; X.-L. Hou, X.-W. Wu, L.-X. Daí, B.-X. Cão and J. Sun, *Chem. Commun.*, 2000, 1195; K. Hiroi, Y. Suzuke and L. Abe, *Tetrahedron: Asymmetry*, 1999, **10**, 1173.
4 G. Mugesh, W.-W. du Mont and H. Sies, *Chem. Rev.*, 2001, **101**, 2125; C. W. Nogueira, G. Zeni and J. B. T. Rocha, *Chem. Rev.*, 2004, **104**, 6255.
5 T. C. Stadman, *Annu. Rev.*, 1996, **65**, 83.
6 J. Lam, H. Breteler, T. Amson, L. Hansen, in *Chemistry and Biology of Naturally-occurring Acetilenes and related Compounds*, Elsevier, Amsterdam, 1988.
7 J. Nakayama and T. Konishi, *Heterocycles*, 1988, **27**, 1731; M. Kuroda, J. Nakayama, M. Hoshino, N. Furusho, T. Kawata and S. Ohba, *Tetrahedron*, 1993, **49**, 3735.
8 T. Y. Ohulchanskyy, D. J. Donnelly, M. R. Detty and P. Prasad, *J. Phys. Chem. B*, 2004, **108**, 8668; M. R. Detty and P. B. Merkel, *J. Am. Chem. Soc.*, 1990, **112**, 3845; Y. Shimizu, K. Oikawa, K.-I. Nakayama and D. Guillon, *J. Mater. Chem.*, 2007, **17**, 4223; M. Lepeltier, J. Hiltz, T. Lockwood, F. Belanger-Gariepy and D. F. Perepichka, *J. Mater. Chem.*, 2009, **19**, 5167.
9 D. L. Boger and R. J. Mathvinink, *J. Org. Chem.*, 1992, **57**, 1429; T. Hiiro, Y. Morita, T. Inoue and H. Kambe, *J. Am. Chem. Soc.*, 1990, **112**, 455; J. Quirante, X. Vila, C. Escolano and J. Bonjoch, *J. Org. Chem.*, 2002, **67**, 2323; S. M. Allin, W. R. S. Barton, W. R. Bowman and T. McInally, *Tetrahedron Lett.*, 2001, **42**, 7887; D. A. Evans, T. Managan and A. L. Rheigold, *J. Am. Chem. Soc.*, 2000, **122**, 11009; M.-L. Bennasar, T. Roca, R. Griera and J. Bosch, *J. Org. Chem.*, 2001, **66**, 7547.
10 G. Heppke, J. Martens, K. Praefcke and H. Simon, *Angew. Chem., Int. Ed. Engl.*, 1977, **16**, 318.
11 (*a*) U. B. Vasconcelos, E. Dalmolin and A. A. Merlo, *Org. Lett.*, 2005, **7**, 1027; (*b*) U. B. Vasconcelos and A. A. Merlo, *Synthesis*, 2006, 1141; (*c*) U. B. Vasconcelos, G. D. Vilela, A. Schrader, A. C. A. Borges and A. A. Merlo, *Tetrahedron*, 2008, **64**, 4619.
12 K. Sonogashira, Y. Tohda and N. Hagihara, *Tetrahedron Lett.*, 1975, **16**, 4467; R. Chinchilla and C. Nájera, *Chem. Rev.*, 2007, **107**, 874; R. Cristiano, D. M. P. O. Santos, G. Conte and H. Gallardo, *Liq. Cryst.*, 2006, **33**, 997; D. M. Price, S. M. Dirk, F. Maya and J. M. Tour, *Tetrahedron*, 2003, **59**, 2497; M. S. Rajendra, R. A. Neves Filho, R. Schneider, A. A. Vieira and H. Gallardo, *Liq. Cryst.*, 2008, **35**, 737; H. Gallardo, R. Cristiano, A. A. Vieira, R. A. Neves Filho and R. M. Srivastava, *Synthesis*, 2008, 605; H. Gallardo, R. Cristiano, A. A. Vieira, R. A. Neves Filho, R. M. Srivastava and I. H. Bechtold, *Liq. Cryst.*, 2008, **35**, 857.
13 A. P. Melissaris and M. H. Litt, *Macromolecules*, 1994, **27**, 883.
14 Some representative examples: B. Ranu and T. Mandayl, *J. Org. Chem.*, 2004, **69**, 5793; A. L. Braga, P. H. Schneider, M. W. Paixão and A. M. Deobald, *Tetrahedron Lett.*, 2006, **47**, 7195; G. Marin, A. L. Braga, A. S. Rosa, F. Z. Galetto, R. A. Burrow, H. Gallardo and M. W. Paixão, *Tetrahedron*, 2009, **65**, 4614; W. Munbunjong,

E. H. Lee, P. Ngernmaneerat, S. J. Kim, G. Sing, W. Chavarisi and D. O. Jang, *Tetrahedron*, 2009, **65**, 2467.
15 P. A. Grieco, Y. Yokoyama and E. Williams, *J. Org. Chem.*, 1978, **43**, 1283; D. Batty and D. Crich, *Synthesis*, 1990, 273; U. Singh, S. K. Ghosh, M. S. Chadha and V. R. Mamdapur, *Tetrahedron Lett.*, 1991, **32**, 255.
16 I. Nishiyama, J. Yamamoto, J. W. Goodby and H. Yokoyama, *J. Mater. Chem.*, 2003, **13**, 2429.
17 W. Weissflog, U. Dunemann, S. Findeisen-Tandel, M. G. Tamba, H. Kresse, G. Pelzl, S. Diele, U. Baumeister, A. Eremin, S. Stern and R. Stannarius, *Soft Matter*, 2009, **5**, 1840.
18 J. M. Viner and C. C. Huang, *Phys. Rev. A: At., Mol., Opt. Phys.*, 1983, **27**, 2763; N. V. S. Rao, T. D. Choudhury, M. K. Paul and T. Francis, *Liq. Cryst.*, 2009, **36**, 409.
19 *Gaussian 03, Revision C.02*, M. J. Frisch, G. W. Trucks, H. B. Schlegel, G. E. Scuseria, M. A. Robb, J. R. Cheeseman, J. A. Montgomery Jr., T. Vreven, K. N. Kudin, J. C. Burant, J. M. Millam, S. S. Iyengar, J. Tomasi, V. Barone, B. Mennucci, M. Cossi, G. Scalmani, N. Rega, G. A. Petersson, H. Nakatsuji, M. Hada, M. Ehara, K. Toyota, R. Fukuda, J. Hasegawa, M. Ishida, T. Nakajima, Y. Honda, O. Kitao, H. Nakai, M. Klene, X. Li, J. E. Knox, H. P. Hratchian, J. B. Cross, V. Bakken, C. Adamo, J. Jaramillo, R. Gomperts, R. E. Stratmann, O. Yazyev, A. J. Austin, R. Cammi, C. Pomelli, J. W. Ochterski, P. Y. Ayala, K. Morokuma, G. A. Voth, P. Salvador, J. J. Dannenberg, V. G. Zakrzewski, S. Dapprich, A. D. Daniels, M. C. Strain, O. Farkas, D. K. Malick, A. D. Rabuck, K. Raghavachari, J. B. Foresman, J. V. Ortiz, Q. Cui, A. G. Baboul, S. Clifford, J. Cioslowski, B. B. Stefanov, G. Liu, A. Liashenko, P. Piskorz, I. Komaromi, R. L. Martin, D. J. Fox, T. Keith, M. A. Al-Laham, C. Y. Peng, A. Nanayakkara, M. Challacombe, P. M. W. Gill, B. Johnson, W. Chen, M. W. Wong, C. Gonzalez, and J. A. Pople, Gaussian, Inc., Wallingford CT, 2004.
20 M. L. Parra, P. I. Hidalgo, E. A. Soto-Bustamante, J. Barbera, E. Y. Elgueta and V. H. Trujillo-Rojo, *Liq. Cryst.*, 2008, **35**, 1251; H. Gallardo, F. R. Bryk, A. A. Vieira, T. E. Frizon, G. Conte, B. S. Souza, J. Eccher, I. H. Bechtold, *Liq. Cryst.* In press; R. Cristiano, H. Gallardo, A. J. Bortoluzzi, I. H. Bechtold, C. E. M. Campos and R. L. Longo, *Chem. Commun.*, 2008, 5134.
21 M. Wahadoszamen, T. Hamada, T. Iimori, T. Nakabayashi and N. Ohta, *J. Phys. Chem. A*, 2007, **111**, 9544; R. Cristiano, E. Westphal, I. H. Bechtold, A. J. Bortoluzzi and H. Gallardo, *Tetrahedron*, 2007, **63**, 2851.
22 V. T. Nikolai, *Optical Spectroscopy: Methods and Instrumentations*, Elsevier Science, 1st edn (June 20, 2006), p. 115.
23 B. Valeur, *Molecular Fluorescence: Principles and Applications*, 2001, Wiley-VCH Verlag GmbH, p. 54.
24 G. A. Crosby and J. N. Demas, *J. Phys. Chem.*, 1971, **75**, 991; S. Fery-Forgues and D. J. Lavabre, *J. Chem. Educ.*, 1999, **76**, 1260.
25 M. Suzuki, T. Sato, A. Kurose, H. Shirai and K. Hanabusa, *Tetrahedron Lett.*, 2005, **46**, 2741.

